Chapter 13

Refractometric Optical Fiber Platforms for Label Free Sensing

Carlos A. J. Gouveia, Jose M. Baptista and
Pedro A.S. Jorge

Additional information is available at the end of the chapter

http://dx.doi.org/10.5772/55376

1. Introduction

The in situ and real time measurement of a variety of chemical and biological parameters is important in diversified environments ranging from industrial processes, medicine to environmental applications. In this context, the demand for novel sensing platforms capable of multiplexing, real time and remote operation in electromagnetic or chemically hazardous environments has increased significantly in recent years.

The combination of fiber optic technology with optical sensing mechanisms has many benefits that make it a promising alternative to standard technologies. Immunity to electromagnetic interferences, small size, and capability for in-situ, real-time, remote, and distributed sensing are some of the most appealing characteristics that motivate a growing scientific community.

Biochemical sensing typically requires that optical signal interacts with the external media, either directly with a given analyte or through an auxiliary membrane, which contains an indicator dye. Some of the most appealing techniques regarding sensitivity and specificity rely on the use of colorimetric or fluorescent indicator dyes. Although some of the intrinsic problems of indicator based sensor like, leaching, photobleaching and temperature dependence have reported solutions, some limitations restrict further developments. A variety of excitation sources, detectors and filters are needed to deal with the large variety of spectral characteristics of dye based sensors. Moreover, these wavelength ranges demand for the use of special optical fibers and optoelectronics, severely limiting its compatibility with the standard telecom optical fiber technology.

In this context, label free optical sensing based on the measurement of refractive index (RI) represents an interesting solution. Such approaches do not interfere with the analyte properties

and require, instead, the design of sensitive layers that experience a refractive index change in its presence. This can be achieved by using biomolecules with a natural affinity to the target, or chemical species having analyte specific ligands. The combination of such membranes with refractive index sensors can therefore provide attractive solutions for biochemical sensing.

The aim of this chapter is to expose the basic principles of evanescent field based fiber optic refractometers, suitable to biosensing field and capable to remote and real time operation. Initially, the principles of the technology are described. Thereafter, recent progress in the area is presented where several fiber optic devices will be detailed, ranging from the popular fiber Bragg gratings, the well known long period gratings, a variety of modal interferometers including tapers, mismatched fiber sections and also multimode interference based structures. Emphasis will be given to the description of the sensing structures and its sensing mechanism, advantages and disadvantages and wherever possible, the sensing performance of each sensing device will be compared in terms of sensitivity and detection limit.

2. Fiber optic refractometers: Principle

Optical fiber consists of a core and a cladding with different refractive indices. The refractive index of the core (n_{core}) is higher than the refractive index of the cladding (n_{clad}). Snell's law can describe the propagation of light in optical fibers by the principle of total internal reflection. In optical fibers, the total internal reflection occurs when light is incident from the core to the cladding, at incident angle (θ_i), greater than the critical angle (θ_c), which can be calculated by the following equation;

$$\theta_c = \arcsin\left(\frac{n_{clad}}{n_{core}}\right)$$

Since light is totally reflected inside the core, no electromagnetic field is propagating in to the cladding. Nevertheless, the electromagnetic field actually penetrates a short distance into the lower refractive index medium, propagating parallel to the interface core-cladding and decaying exponentially with the distance from the interface (See figure 1). The physical explanation for this phenomenon is that when applying Maxwell equations to the interface between two dielectrics, the tangential components of both the electric and magnetic fields must be continuous across the interface, this is, the field in the less dense medium cannot abruptly become zero at the interface and a small portion of light penetrates into the reflecting medium. This boundary condition can only be satisfied if the electromagnetic field crosses the interface, creating the so-called evanescent wave [1]. The penetration depth (d_p) of the evanescent wave is a key parameter for sensing purposes. It is the distance from the interface at which the amplitude of the electric field is decreased by a factor equal to *1/e* and, following the approximation of geometrical optics, it can be expressed by the following equation:

$$d_p = \frac{\lambda_0}{2\pi} \frac{1}{\sqrt{n_{core} \cdot \sin_2(\theta_i) - n_{clad}}}$$

where λ_0 is the radiation wavelength. The penetration depth of the evanescent field varies from 50 nm to 1000 nm depending on the wavelength, the refractive indices and the angle of incidence.

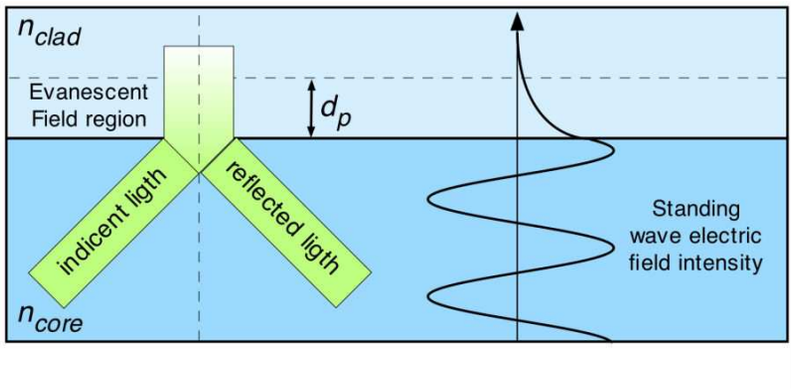

Figure 1. Evanescent field in the core/cladding interface of an optical fiber

The majority of the fiber refractometers are based on evanescent field interactions. However, fibers were originally designed for optical communications. A typical single mode optical fiber has a core diameter between 8 and 10.5 μm, a cladding diameter of 125 μm and light propagates confined in the core. Therefore, the penetration depth is far smaller than the cladding thickness and there is almost no interaction between the optical signal and the external medium. Strategies must be devised in order to provide interaction with the surrounding medium. Typically, the evanescent field can be exposed by removing partially or totally the cladding of the optical fiber. This can be done by chemical etching, tapering or side polishing techniques. In alternative, it is possible to use specific tools capable to transfer energy from the fundamental core mode to cladding modes. Fiber gratings are an example of these devices. In such a cases the optical radiation can interact with the external environment due to the evanescent field formed at the cladding/external medium interface. In this case, the penetration depth is given by:

$$d_p(m) = \frac{\lambda_0}{2\pi \cdot n_{clad}} \frac{1}{\sqrt{\sin^2(\theta_{(m)}) - \sin^2(\theta_{c'})}}$$

where $\theta(m)$ is the incident angle of the geometrical ray associated with the *mth* cladding mode and $\theta_{c'}$ is the critical angle at the interface between the fiber cladding and the external environment. Clearly, $\theta(m)$ is different for each cladding mode and decreases with the increment of the order of the cladding mode. It is important to observe that the *dp* changes as a function of the coupled cladding mode as well as of the external refractive index. The dependence of *dp* on the external refractive index (n_{ext}) is implicitly contained within $\theta_{c'}$, which can be expressed as:

$$\theta_{c'} = \arcsin\left(\frac{n_{ext}}{n_{clad}}\right)$$

Fiber optic biochemical sensors based on evanescent field configurations rely on the use of sensing layers deposited on the sensitive surface that experience a refractive index change in presence of an analyte. This can be achieved by using biomolecules with a natural affinity to the target, or chemical species having analyte specific ligands. When exposed to an analyte, a chemical/biochemical interaction takes place within this layer or on its surface. In this case, only a portion of the optical radiation which comes out of the sensor (evanescent field) is modulated, depending on the thickness of the interaction region.

Biological sensing is based on the specific binding between biorecognition molecules (antibodies, oligonucleotides, aptamers or phages) immobilized on the sensor surface and the targeted biological species, which causes a change in the effective thickness or density of the surface of fiber and consequently a change on the optical signal. Figure 2 conceptually shows an example of label free fiber optic biosensor. A functional coating is used to support and enhance the attachment of the bioreceptor molecules, which bind the analyte [2].

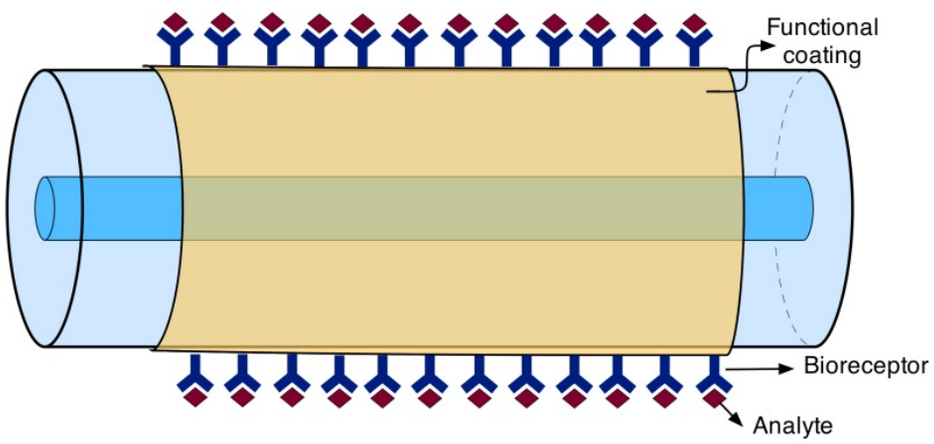

Figure 2. Label free fiber optic biosensor schematic representation

In the following sections the most relevant fiber refractometric platforms based on evanescent field interactions and capable for label free biochemical sensing will be presented, including their measurement principle and some examples of most important works presented till now.

3. Fiber Bragg gratings

Fiber Bragg grating (FBG) sensors have generated great interest in recent years because of their many industrial and environmental applications. FBGs are simple, versatile, and small intrinsic sensing elements that can be written in optical fibers and which consequently have all the advantages normally attributed to fiber sensors. In addition, due to the fact that typically the measurand information is encoded in the resonant wavelength of the structure, which is an absolute parameter, these devices are inherently self-referenced. Moreover there are several

intrinsic advantages associated with FBG technology such as reflection operation mode, narrowband spectral response and their compatibility with standard telecom technology, therefore can be easily multiplexed, which is particularly important in the context of remote, multi-point and multi-parameter sensing [3]. Based on diffraction mechanism, they consist on the periodic perturbation of the core of the optical fiber (typically half-wavelength) that is induced by exposing the fiber to an interference pattern of UV light or femtosecond radiation. They are characterized by the periodicity Λ of the refractive index modulation and by the effective refractive index of the waveguide mode $n_{eff.}$ The grating constitutes a wavelength selective mirror or rejection filter defined by the Bragg resonance wavelength (λ_B)

$$\lambda_B = 2n_{eff}\Lambda$$

The full width at the half maximum (FWHM) of the resonant peak of the Bragg grating is typically a few hundred picometers. It depends on the physical length of the grating, which is usually few millimeters. Figure 3 illustrates the principle of operation of an FBG. When a broadband optical signal reaches the grating, a narrow spectral fraction is reflected and the remaining is transmitted. The peak wavelength of the reflected signal is defined by the Bragg resonance wavelength.

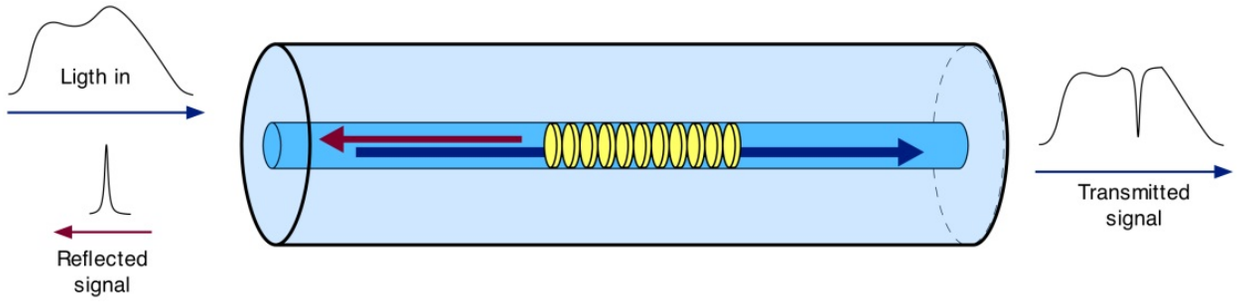

Figure 3. Operation principle of fiber Bragg grating

FBG sensors have been widely used for strain and temperature measurement [4]. Bragg gratings works mainly with radiation confined to the fiber core, this way strategies have to be devised in order for the radiation to interact with the external medium. Typically, FBG based refractometers rely on the evanescent field of the core modes under fiber etching conditions, which enables interaction with the surrounding medium.

The first demonstration of an FBG as a refractometer was done in 1997 by Asseh *et al.* [5], and it was based on the application of chemical etching to the fiber region where the grating was located. The etching process was done by immersing the fiber in a solution of 40% hydrofluoric acid (HF) for approximately 50 min. After etched, the fiber had a diameter of 11μm; thus 1μm of cladding still remained. The sensor was tested in different solutions of sucrose, inferring a variation of refractive index between 1.333-1.345 RIU. The estimated sensibility was 1nm/RIU and the measured resolution was $\pm 5\times10^{-4}$ RIU. Figure 4 illustrates an FBG based refractometer,

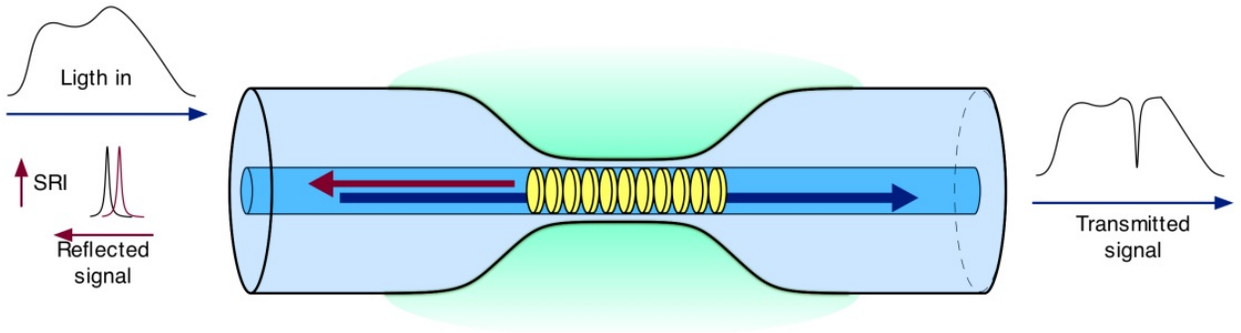

Figure 4. Etched fiber Bragg grating refractometer

when the cladding of the optical fiber was partially etched. Thus, the wavelength of the reflected signal depends on the external refractive index.

Regarding sensitivity enhancement and temperature compensation, in 2001 Schroeder *et al.* [6] presented a two in-line FBGs written on a single-mode depressed-cladding optical fibre of cut-off wavelength 750 nm. One of the gratings was side-polished to become sensitive to the SRI and the second one for thermal compensation. The effect of high refractive index overlays was studied in order to shift the mode field to the surface of the sensor and to enhance the sensitivity for low refractive index analytes. Operation in wavelengths far above the cut-off wavelength was also explored resulting in an improvement of the sensitivity of the sensor. The sensor was tested in different solutions, inferring a variation of refractive index between 1.30-1.46 RIU. The maximum sensitivity for an external refractive index close to 1.45 was found to be 300nm/RIU and the measured resolution was $\pm 2\times10^{-6}$ RIU.

A simpler solution for thermal compensation was published by Iadicicco *et al.* (2005), a single grating half-etched for simultaneous measurement of refractive index and temperature. The operation principle relies on the splitting of the original grating spectral response in two different peaks due to a selective etching over the grating length, where one of them becomes sensitive to the external refractive index and the other one is just sensitive to temperature [7]. Concerning enhancements in sensitivity, in 2005 Chryssis *et al.* [8] has shown that an effective solution is provided by etching the core of a fiber Bragg grating. A maximum sensitivity of 1394 nm/RIU is achieved as the surrounding index approaches the core index when the residual diameter was reduced to 3.4μm.

In the past few years, microfibers have attracted increasing interest due to their intrinsic advantages such as large evanescent field, small effective mode field diameter and low-loss interconnection to single mode fibers. Microfibers can be produced by the use of standard flame brushing technique. Bragg gratings written in microfiber have been also explored for refractive index sensing. In 2010 Fang *et al.* [9] presented FBGs written in microfibers with diameters ranging from 2μm to 10μm by using femtosecond pulse irradiation. The maximum sensitivity obtained was 231.4 nm/RIU for refractive index values near 1.44 for a microfiber with 2μm diameter. However, femtosecond laser Bragg grating inscription relies in the physical deformation of the fibre surface, which can weaken even more the micrometric structure. Concerning with this fact, later in the same year, Zhang *et al.* [10] demonstrated a

http://dx.doi.org/10.5772/55376

microfiber Bragg grating fabrication using a KrF excimer laser in a highly Ge-doped photosensitive microfibers with diameters of 6 and 6.5μm, respectively. Two reflection peaks were observed in the spectrum of FBG. The reflected peak induced by the higher-order mode was used to monitor RI variations, because the higher-order mode has a larger evanescent field outside the microfiber and thus it is more sensitive to the surrounding refractive index, compared with the fundamental mode reflection. The other peak was used for temperature referencing. The maximum sensitivity was ~102 nm/RIU at a refractive index of 1.378, in the 6μm diameter fiber.

Etched FBG, side polished FBG or microfiber Bragg gratings are interesting devices that exploit the influence of the surrounding refractive index (by the evanescent field interaction) on the effective index of the core mode, and consequently on the Bragg wavelength (λ_B). However, in order to enable the interaction with the external medium, the fiber diameter should be reduced, removing the cladding and in some cases partially the core. The sensitivity of the FBG is highly dependent on the diameter of the fiber in the region of the grating. Nevertheless, this process introduces fragility in the fibre sensor especially in cases where maximum sensitivity is required.

A different approach to develop fiber optic refractometers based on FBG technology was proposed in 2001 by Laffont *et al.* [11]. The sensing configuration relies on the use of tilted FBG (TFBG) as refractive index sensors by using the transmission spectrum changes due to the cladding modes resonances sensitivity to the external medium. In TFBGs the modulation pattern is blazed (tilted) by an angle θ with respect to the fiber axis. This asymmetry enables the coupling to circularly and non-circularly symmetric contra-propagating cladding modes and reduces the energy coupling to the contra-propagating core mode. The cladding modes are guided by the cladding boundary, and as a result, their effective index depends on the external index. The sensitivity of the cladding to variations of the SRI increases with mode order, since the penetration depth of the evanescent field increases for higher-order modes. With the increment of the SRI, the center wavelength of the resonances experienced a shift to higher wavelengths. In addition to their spectral shift, the intensity drops progressively, to fit a smooth loss curve. Thus, monitoring the shifts of the cladding modes relative to the Bragg resonance or measuring the normalized envelope of the cladding mode resonance spectrum in transmission can held an accurate measure of the surrounding refractive index. Figure 5 shown a conceptual representation of a tilted FBG.

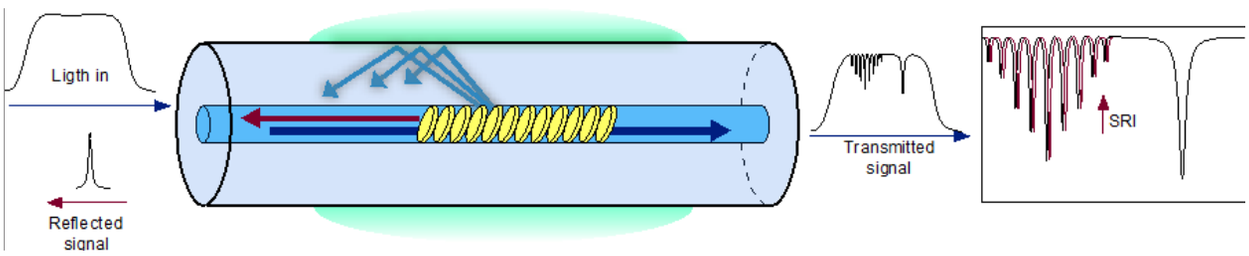

Figure 5. Refractometer based on a tilted fiber Bragg grating

The TFBGs used in the experiment of Laffont *et al.* [11] were written in a standard single mode fiber using a Lloyd mirror interferometer. The measurement of SRI was based on the normalized envelope of the cladding mode resonance spectrum in transmission. It was also shown that this parameter was relatively insensitive to temperature. Another reason for using the envelope of the resonance spectrum is that, choosing the proper tilt angle, this parameter can change monotonically and smoothly for refractive index values between 1.32 and 1.42, with a small change in sensitivity. Using the normalized area parameter and a 16° TFBG a resolution of $\pm 10^{-4}$ RIU was achieved. In 2007 Chan *et al.* [12] proposed a relative measurement of refractive index, based on the separation distance between certain cladding modes that were dependent on the refractive index and temperature and the core mode, which is refractive index independent. A 4° TFBG was used where refractive index sensitivity of 10 nm/RIU was obtained, achieving a resolution of $\pm 10^{-4}$ RIU.

TFBGs are a suitable option for refractometric sensing in terms of performance and robustness of the fiber structure. However, a TFBG couples the core mode to a number of cladding modes in a large wavelength bandwidth, which renders difficult the signal readout and multiplexing. In addition, the fact that the measurement must be made in transmission, requiring access to the sensor from both sides, can represent a difficulty in some applications. Recently a few authors have been exploring the possibility to excite the cladding modes of standard FBG by transferring power from the fundamental core mode to the cladding modes in the upstream of the FBG. Thereby, the FBG will couple back the light to the fundamental core mode. This arrangement enables the possibility to read the cladding mode of the Bragg grating in the reflected spectrum

In 2010 Han *et al.* [13] have shown for first time this method with concatenating a LPG and a FBG. The LPG partially couples light from the core mode to a cladding mode, both of which are reflected by the FBG. The refractive index sensitivity of 2.3 nm/RI was obtained. Recently, based on the same principle, Wu *et al.* [14] presented a singlemode–multimode–singlemode fiber structure (SMS) assisted FBG to measure the SRI. This structure utilizes multimode fiber to excite cladding modes of an FBG written on the singlemode fiber and recouple reflected cladding modes to the input singlemode fiber. The maximum achieved sensitivity was 7.33 nm/RIU in the range from 1.324 to 1.439 RIU. Fiber refractometers based in cladding modes of standard FBGs represent an interesting opportunity for label free sensing, especially by using all-grating devices which enable the possibility of efficiently transfer power to specific high order modes in order to excite specific cladding modes of an FBG. However, work is still to be done concerning the enhancement of sensitivity, which is still far from ideal.

Owing to reflective nature of this devices a few FBG based Fabry-Perot cavities were presented for refractive index measurement. In 2005 Liang *et al.* [15] reported a refractive index sensor based on an etched fiber Fabry-Perot interferometer with a radius of 1.5μm. The sensor showed a sensitivity of 71.2 nm/RIU and a variation of refractive index of $\pm 1.4 \times 10^{-5}$ can be detected. Table 1 summarizes the most relevant FBG based refractometers presented to date and their performance parameters.

Configuration	Measurement method	Year	RI Range	Sensitivity	Resolution	Ref.
Etched FBG	Spectral Shift	1997	1.333-1.345	1 nm/RIU	5×10^{-4}	[5]
	Spectral Shift	2005	Near 1.44	1394 nm/RIU	$7.2\times10^{-6\,(*)}$	[8]
Polished FBG	Spectral Shift	2001	Near 1.45	300 nm/RIU	$10^{-6(*)}$	[6]
Microfiber FBG	Spectral Shift	2010	Near 1.44	230 nm/RIU	$5\times10^{-6(*)}$	[9]
	Spectral Shift	2010	Near 1.38	102 nm/RIU	$10^{-5(*)}$	[10]
TFBG	Normalized Area	2001	1.32-1.42		10^{-4}	[11]
	Spectral Shift	2007	Near 1.32	11.2 nm/RIU	10^{-4}	[12]
LPG/FBG	Spectral Shift	2010	Near 1.45	2.32 nm/RIU	$10^{-4(*)}$	[13]
MMF/FBG	Spectral Shift	2010	1.40-1.44	7.33 nm/RIU	$10^{-4(*)}$	[14]
FP-FBG	Spectral Shift	2005	Near 1.33	71.4 nm/RIU	1.4×10^{-5}	

(*) Theoretical maximum resolution given by the ratio between the readout device resolution and refractive index sensitivity of the sensor.

Table 1. Comparison of the characteristics of the most relevant FBG based refractometers

3.1. Applications

Several FBG based refractometers have been described rely on the measurement of the refractive index changes for the measurement of sucrose, salt, ethylene glycol, Isopropyl Alcohol among others [5-7]. Using functional layers just few works were presented. The first demonstration of the concept of biosensor based on FBG, was done by Chryssis *et al.* (2005) [16], based on an etched FBG, where single stranded DNA oligonucleotide probes of 20 bases were immobilized on the surface of the fiber grating using relatively common glutarahyldehyde chemistry. Hybridization of a complimentary target single strand DNA oligonucleotide was monitored in situ and successfully detected. Later, in 2008 Maguis *et al.* [17] presented a biosensor based on a TFBG refractometer that enables to directly detect, in real-time, target molecules. Thus, bovine serum albumin (BSA) (antigen) and anti-BSA (antibody) were used to study the reaction kinetics of the antigen- antibody recognition by changing the antibody concentration in the different configurations for the antigen immobilization.

4. Long period fiber gratings

A Long period grating (LPG) is one of the most popular fiber optic refractive index sensor and it has been widely used for chemical and biological sensing. Like FBG, LPG is also a diffraction structure, where the refractive index of the fiber core is modulated, with a period between 100μm to 1000μm that is induced in the optical fiber using different techniques: UV laser irradiation, CO_2 laser irradiation, electric-arc discharge, mechanical processes and periodic etching [18]. This periodic perturbation satisfies the phase matching condition between the fundamental core mode and a forward propagating cladding mode of an optical fiber. Thereby,

in an LPG, the core mode couples into the cladding modes of the fiber, resulting in several attenuation bands centered at discrete wavelengths in the transmitted spectrum, where each attenuation band corresponds to the coupling to a different cladding mode. The spectral width of the resonant dip varies from few nanometers up to tens of nanometers depending on the physical length of the grating.

LPGs are intrinsically sensitive to external refractive index exhibiting changes in the position of the resonance wavelength. The resonant wavelength of light coupling into a particular cladding mode is given by the phase matching condition [19]:

$$\lambda_{res}^{m} = \left(n_{eff,core} - n^{m}_{eff,clad}\right)\Lambda$$

Where Λ is the grating period, $n_{eff,core}$ and $n^{m}_{eff,clad}$ are the effective indexes of the core and mth-cladding mode, respectively. Following the phase matching condition, a change in the surrounding refractive index will induce a shift in the resonance wavelength due to the variation of the $n^{m}_{eff,clad}$, which is dependent on the external refractive index. The first long period grating inscribed successfully in an optical fiber was reported in 1996 by Vengsarkar *et al.* [20] for band-rejection filters, and in the same year Bhatia *et al.* [21] presented the first application of long period gratings for refractive index sensing, reporting a wavelength shift of 62nm for a refractive index change between 1.40-1.45 and an average resolution of ± 7.69×10^{-5} RIU in the same range; for an LPG with period of 320μm written by UV radiation exposition in a Corning standard 1310nm fiber. Figure 6 illustrates the principle of operation of long period gratings.

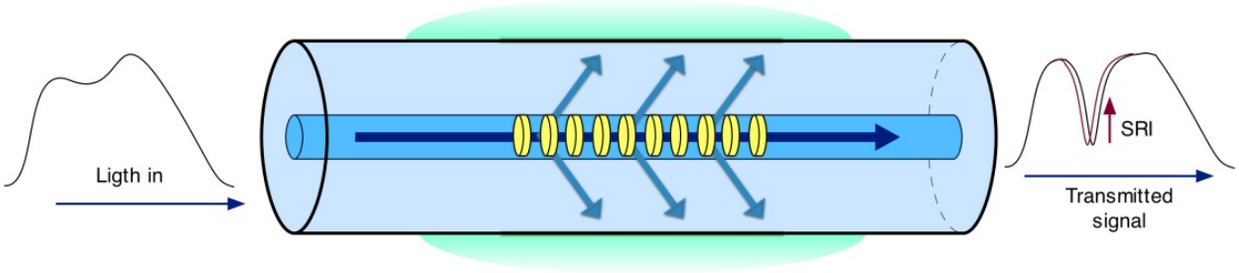

Figure 6. Fiber long period gratings

Shu *et al.* [22] reported in 2002 a Long Period grating written in B–Ge co-doped fiber by UV laser irradiation technique, with a period of 202μm. For the eleventh order mode, a refractive index sensitivity of 1481 nm/RIU was shown in the range between 1-1.36 RIU, which is according with our knowledge the best sensitivity for a bare LPG reported for this range. Electric-arc induced LPGs are attractive due to its simplicity and flexibility, as well as the low cost of the fabrication process and its applicability not only to commonly used photosensitive fibers, but also to photonic crystal fibers, which are made of pure silica. In 2011 Smietana *et al.* [23] published a work on gratings with periods of 345 and 221μm, respectively, for LPGs based on the SMF28 and PS1250/1500 fibers. Which are the shortest periods achieved for this

type of fibers using the electric-arc manufacturing technique. Results showed refractive index sensitivities of 302 and 483 nm/RIU in the range between 1.33-1.41 that represent also the highest sensitivity reported for a bare LPG made by electric-arc technique for the specified measuring range.

The sensitivity of an LPG is then typically defined as a shift of the resonance wavelength induced by a measurand. The sensitivity characteristic of a bare LPG to surrounding refractive index changes has an increasing (in modulus) non-linear monotone trend. The result is that the maximum sensitivity is achieved when the external index is close to the cladding index while for lower refractive indices (around 1.33) the LPG is scarcely sensitive. Figure 7 shows the behavior of resonance wavelength and its optical power to refractive index changes. The behavior changes when a thin layer of sub-wavelength thickness (few hundreds of nanometers) and with higher refractive index than the cladding is deposited thereon. The use of high refractive index (HRI) overlays in fiber optic sensors refractometers based on evanescent wave was explored initially by Schroeder *et al.* [6] for a polished FBG. Coated LPGs with thin HRI layers was firstly proposed by Rees *et al.* [24] and since then, several authors have explored its use for LPG RI sensitivity enhancement [24-28] and to develop highly sensitivity chemical devices [29, 30].

The HRI overlay draws the optical field towards the external medium extending its evanescent wave. As a result there is an increased sensitivity of the device to the surrounding RI. Due to the refractive-reflective regime at the cladding-overlay interface, the cladding modes in a HRI coated LPG are bounded within the structure comprising the core, the cladding and the overlay. This means that a relevant part of the optical power carried by the cladding modes is radiated within the overlay. The field enhancement in the overlay depends strongly on the overlay features (thickness and refractive index) and the SRI. For a fixed overlay thickness and refractive index, by increasing the SRI, the transition from cladding to overlay modes occurs: the lowest order cladding mode (cladding mode with highest effective refractive index) becomes guided into the overlay. At the same time, the higher order modes move to recover the previous effective indices distribution. This is reflected through the phase matching condition in the shift of each attenuation band toward the next lower one [31]. Resulting from this modal transition that the attenuation bands can exhibit a sensitivity of thousands of nanometers per refractive index unit.

Pilla *et al.* [32] reported in 2009 a polystyrene coated LPG ($\Lambda = 460\mu m$). For a 5^{th} order resonance, sensitivities of ~ 5000 nm/RIU (near 1.41) and ~ 2500 nm/RIU (near 1.38) were achieved for coating thicknesses of 270nm and 320nm, respectively. The reported data showed how by changing the overlay thickness it is possible to tune the sensitivity characteristic for the considered cladding mode in the desired refractive index.

High order cladding modes that strongly penetrate the external medium, on the other hand, offer higher sensitivity, and obviously these are the most desirable for sensing purposes. An increase in the order of the coupled cladding mode is obtained by decreasing the grating period [33]. Pilla *et al.* [34] reported recently in 2012 a polystyrene coated LPG ($\Lambda = 200\mu m$). The coating thickness was approximately 245nm. For an 11^{th} order resonance, sensitivity over 9000 nm/RIU near 1.347 was achieved, which is so far the best sensitivity obtained for a fiber device

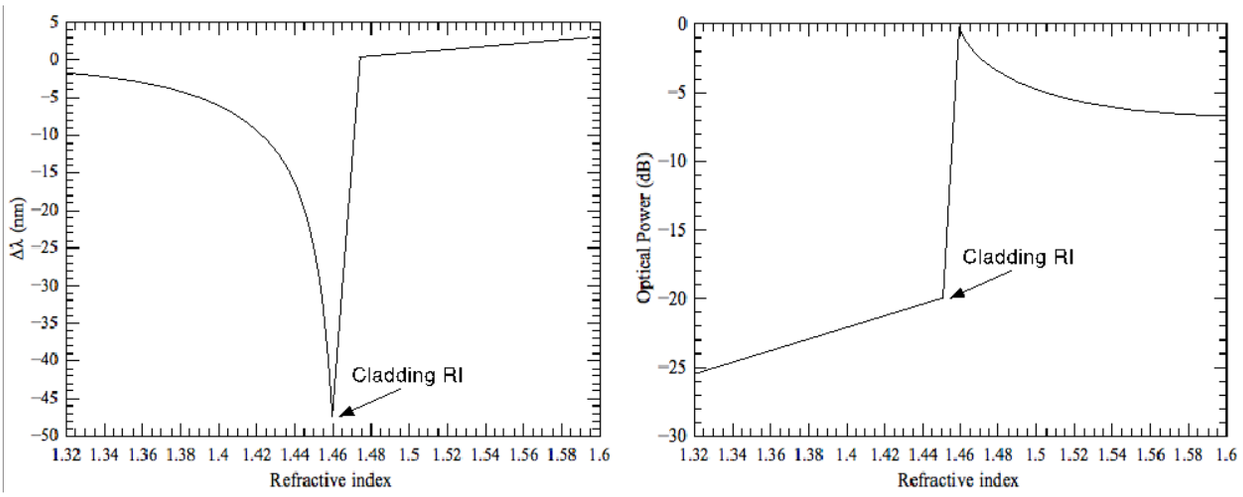

Figure 7. Refractive index response of a LPG

for this range of RI. This result shows HRI coated LPGs as a promising technology for a high-performance label free sensing applications.

LPGs show great sensitivity to the surrounding RI, but also at the same time to temperature. In the other hand, the measurement of the refractive index is strongly dependent on the temperature due to the thermo-optic coefficient. Thus, measurement and compensation of this parameter is an important issue for this kind of platforms. A number of techniques have been proposed in order to get rid of the temperature cross-sensitivity mainly based on the use of a second grating sensitive only to temperature [35, 36].

LPG based interferometers have shown higher resolution to refractive index measurement compared to the use of a single LPG. The advantage of using those structures lies on their interferometric nature and its principle of operation, where the coupled core and cladding modes from one LPG combine again at a second matched LPG to form interference fringes. The core and cladding paths constitute the arms of an all fiber Mach–Zehnder interferometer (see figure 8) [37]. In 2002, Allsop *et al.* [38] presented an LPG based Mach-Zehnder as a refractometer. Using a pair of LPG (Λ = 270μm) apart 100mm from each other, coupling 9th order cladding mode and interrogated by phase generated carrier technique; a resolution of $\pm 1.8\times10^{-6}$ was achieved for a RI range between 1.37-1.40. Later, in 2004 Swart *et al.* [39] presented a refractometer based on Michelson interferometer, by using a single LPG located 45 mm away from the mirrored tip (see figure 9). Compared with the Mach-Zehnder layout, the presented configuration has potential advantages such as reflection operation and compactness, it just need half interaction path length for the same sensitivity.

More recently, in 2010 Mosquera *et al.* [40], presented an optical fiber refractometer based on a Fabry–Perot resonator that incorporates an intracavity long-period grating that couples and recovers energy to the fiber cladding after being phase shifted by the surrounding refractive index. Figure 10 shows the sensing head configuration. The resonator is formed by two high reflectivity (~ 95%) FBGs separated by 47.5 mm. The external refractive index is monitored by the resonant frequencies of the Fabry–Perot interferometer, which can be measured either in transmission or in reflection. Results give a detection limit of $\pm 2.1\times10^{-5}$ RIU at n=1.33.

http://dx.doi.org/10.5772/55376

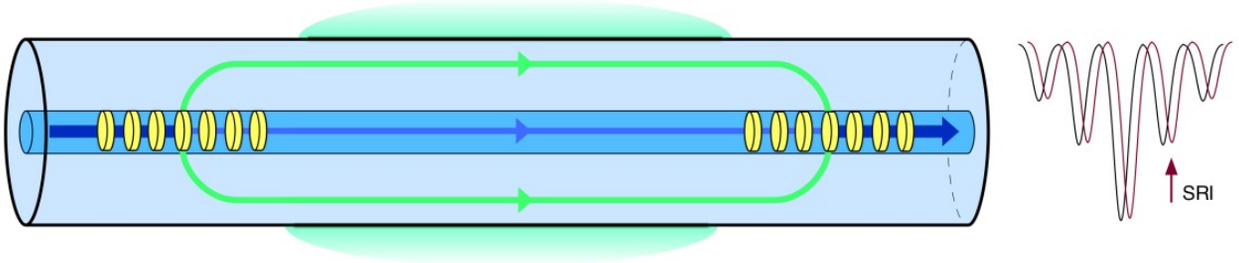

Figure 8. All fiber LPG based Mach-Zehnder interferometer

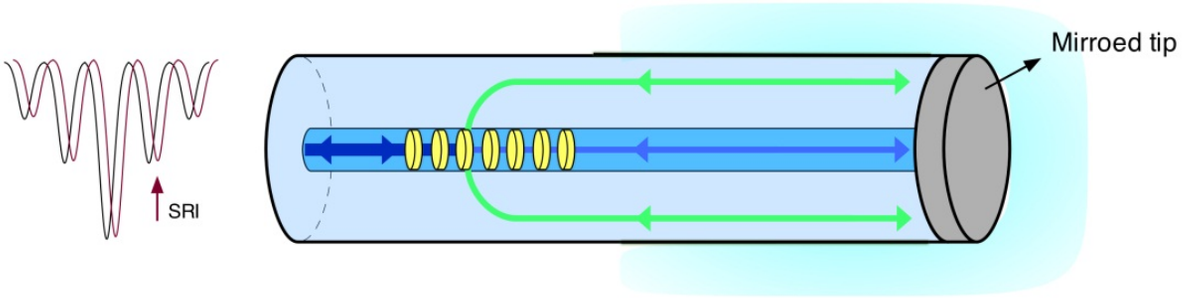

Figure 9. All fiber LPG based Michelson interferometer

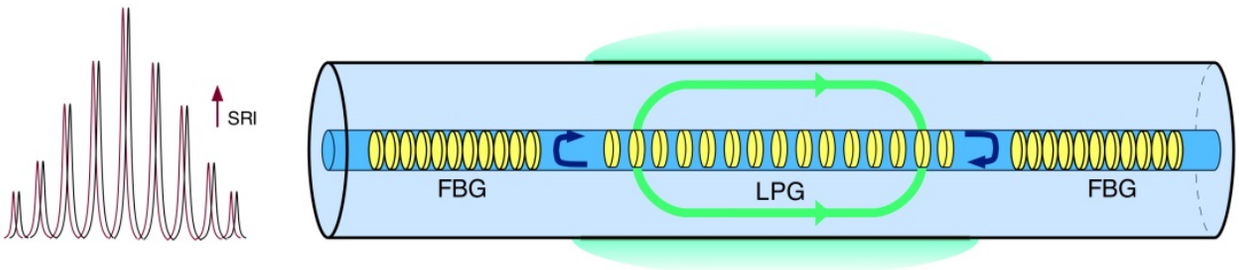

Figure 10. Intracavity LPG Fabry-Perot resonator

4.1. Applications

Long period gratings are the most popular fiber optic sensor for label free sensing, since in 1996 Bhatia *et al.* [21] presented the first LPG based refractometer, many refractive index sensors have been reported along the years, using the refractometric ability to measure parameters such as the concentration of ethylene glycol, sucrose, salt, ethanol among others [33, 41-46]. Although this approach is not the most reliable due to the possible interference of other species present in the solution, which are different from the analyte of interest. Thus, the deposition of sensitive thin layers that can change their own refractive index in presence of a specific analyte have opened a very interesting niche of applications. However, as mentioned

above, the thickness and refractive index of the overlay are critical aspects that strongly affect the sensitivity of the device.

LPGs coated by functional layers have been successfully exploited for chemical sensing. Gu *et al.* [30] reported a LPG with a sol-gel derived coating of SnO_2 with optimized thickness. In presence of specific gases, the semiconductor surface energy changes, which leads to the change of conductivity and refractive index. The sensor was tested for Ethanol vapor detection. Corres *et al.* [29] used the electrostatic self-assembled method to create pH sensitive films with an optimal overlay thickness. Two coatings were presented. The first one is based on polyallylamine hydrochloride (PAH), polyacrylic acid (PAA), and the second one was done incorporating the pigment Prussian blue (PB) in the PAH/PAA matrix. Faster response was obtained with the introduction of PB particles in the polymeric matrix. Barnes *et al.* [47] presented a LPG functionalized with a polymethylsiloxane coating; able to perform solid-phase microextraction of organic solvents such as xylene and cyclohexane. The grating was interrogated using cavity ring down spectroscopy. Improvements regarding with sensitivity and miniaturization of the sensing probe were studied recently by the same authors [48]. An LPG coated with a zeolite thin film was used to detect the presence of toluene and isopropanol vapors by Zhang *et al.* [49].

Recently, Korposh *et al.* [50] reported a LPG multilayer film from silica nanoparticles and the subsequent infusion of a porphyrin into the porous coating for ammonia sensing. The infusion of a functional material into the base mesoporous coating, chosen to be sensitive to a specific analyte, represents the novelty of this work. Two possible sensing mechanisms were shown, based upon changes in the refractive index of the coating. Chemically induced refractive index changes of the mesoporous coating at the adsorption of the analyte to the functional material (PAA), and chemically induced desorption of the functional material (tetrakis-(4-sulfophenyl)porphine), from the mesoporous coating.

LPG has been widely used for biochemical sensing; on this case a biomolecule with affinity to a target can be used as functional coating. The earliest demonstration of biomolecule detection using this structure was done by DeLisa *et al.* [51], where the LPG was used for sensitive detection of antibody-antigen reactions. Goat anti-human Immunoglobulin G (antibody) was immobilized on the surface of the LPG, and detection of specific antibody- antigen binding was shown. Later, several works were reported regarding antibody-antigen interaction [32, 52-59] and also DNA hybridization [58, 60-62].

LPGs applied for label free detection of specific bacteria using physically adsorbed bacteriophages were presented for the first time by Smietana *et al.* [63], where T4 phages immobilized onto the surface of an LPG were used as recognition element for *E. Coli* detection. Recently, improvements in sensitivity in a similar work was presented by Tripathi *et al.* [64].

Lately, an enzyme coated LPG was used for glucose detection by Deep et al [65]. The authors demonstrated the successful immobilization of glucose oxidase on to the 3-aminopropyltriethoxysilane (APTES) silanized LPG fibers for the development of a new glucose sensing technique.

5. Modal interferometers

Fiber modal interferometers have recently concentrated the focus of research because of their potential sensing capabilities and in some cases the reduced cost and simplicity of fabrication. In the previous section an LPG based modal interferometer was introduced. The LPGs were used as mechanism to couple light from core to cladding and subsequently from cladding to core. There are different mechanisms through which the high order modes could be selectively excited, by tapering a single mode optical fiber, through a core diameter mismatching structure (larger or thinner) or by a simple misaligned splice. Other kind of devices relies on multimode interference, in such a cases a small section of multimode fiber is properly inserted between single-mode fibers. The aim of this section is to describe the sensing mechanism of this kind of devices and to address the most relevant contributions for chemical and biosensing field.

5.1. Tapered single-mode fiber

Tapering a single mode fiber involves reducing the cladding diameter along with the core and it is made by heating a section of the fiber and pulling on both ends of the fiber in the opposite directions, either under a constant speed, force or tension. The heat source can be a gas burner flame, a focused CO_2 laser beam or an electric arc formed between a pair of electrodes. When the optical fiber is tapered, the core–cladding interface is redefined in such a way that the light propagation inside the core penetrates to the cladding and it is confined by the external medium.

A fiber taper consists of three contiguous parts: one taper waist segment with small and uniform diameter, and two conical transition regions with gradually changed diameter. Depending on the pulling conditions it is possible to fabricate tapers with different shapes and properties. Fiber tapers may be divided into two distinct categories: adiabatic and non-adiabatic. An adiabatic fiber taper is characterized by a very smooth change in the profile (small taper angle) in order to ensure a smooth mode conversion without significant losses in the transmitted signal. In this case, the main portion of the radiation remains in the fundamental mode (LP_{01}) and does not couple to higher order modes as it propagates along the taper.

On the other hand, non-adiabatic fiber tapers (abrupt taper angle) can be done in such a way that coupling occurs primarily between the fundamental mode of the un-pulled fiber and the first two modes of the taper waveguide (LP_{01}, LP_{02}), where due to the large difference of the refractive indexes of air and fiber cladding, the taper normally supports more than one mode. The light propagates at the air/cladding interface of the tapers waist region in which case the single mode fiber is converted into a multimode waveguide. The result of back and forth coupling between the single mode of the fiber and the two (or more) modes of the taper is an oscillatory spectral response. The efficiency of this last coupling is dependent on the relative phase of the participating modes. Therefore, this device behaves as Mach-Zehnder modal interferometer. When there are only two modes, the relative phase is $\Delta\varphi=\Delta\beta L$, where $\Delta\beta$ and L are the difference in propagation constants of the two modes and the interaction length along the taper, respectively. Therefore, the spectral response of the taper will shift correspondingly by changing the above terms. For instance, if the refractive index of the surrounding environ-

ment of the taper changes, the difference in propagation constants and the relative phase would be modified leading to a shift of the spectral response. Usually, this devices present waist diameter of few microns, promoting high interaction of the optical signal with the surrounding medium; thereby they are very sensitive to SRI. Figure 11 shows conceptually a non adiabatic (abrupt) fiber taper.

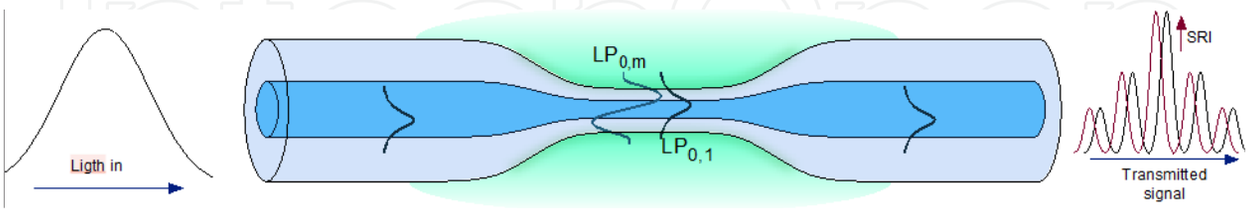

Figure 11. Abrupt taper based refractometer

Fiber refractometer based in non-adiabatic tapers has been proposed recently as platform for label free sensing. Zibaii *et al.* [66] presented a single-mode non-adiabatic tapered optical fiber sensor for sensing the variation in refractive index with concentration of D-glucose in deionized water and measurement of the RI of amino acids (AAs) in carbohydrate solutions. This method showed a rewarding ability in understanding the basis of biomolecular interactions in biological systems. The fiber tapers were fabricated using heat-pulling method with waist diameter and length of 7μm and 9mm respectively. The limit of detection of the sensing probe was 55 ppm for a D-glucose concentration ranging from 0 to 80 mg ml^{-1}. Regarding refractive index measurements a sensitivity of ~ 1150 nm/RIU in the range between 1.3330 - 1.3447. A resolution of $\pm 8.2\times10^{-6}$ RIU was also calculated. Zibaii *et al.* [67] presented also a similar sensing probe for real-time monitoring of the Escherichia coli (E. coli K-12) growth in an aqueous medium. The taper length and waist diameter were 7-9μm and 3nm respectively. The bacteria were immobilized on the tapered surface using Poly-L-Lysine. By providing the proper condition, bacterial population growth on the tapered surface increases the average surface density of the cells and consequently the refractive index of the tapered region would increase. The adsorption of the cells on the tapered fiber leads to changes in the optical characteristics of the taper. This affects the evanescent field leading to changes in optical throughput. Concerning improvements in refractive index sensitivity the same author showed a single-mode non-adiabatic tapered optical fiber sensor inserted into a fiber loop mirror. Adjusting the polarization controllers inserted in the loop allowed to excite different cladding modes in the interferometric taper resulting in different optical paths for the clockwise and the counterclockwise beams. The variation of the polarization settings provided a tuning in the RI sensitivity in a range between 800nm/RIU - 1200 nm/RIU for indices in the range from 1.3380 to 1.3510 [68].

Later, Tian *et al.* [69] published a tapered optical fiber biosensor that enables the label-free detection of biomolecules. The biomolecules bonded on the taper surface were determined by demodulating the transmission spectrum phase shift. The taper waist diameter and length

were approximately 10μm and 12mm, respectively. A tapered optical fiber biosensor was fabricated and evaluated with an Immune globulin G antibody-antigen pair.

5.2. Core mismatch

Abrupt Tapered devices show high sensitivity to refractive index measurements. However, after the tapering, due to reduced fiber diameter, the structure becomes very fragile and special handling is needed. Recently, a different approach based on core mismatched sections have been investigated. In this case, mismatched sections are proposed as valid alternatives as mode-coupling mechanisms to transfer optical power between core and cladding modes in optical fiber. The idea is to couple and recouple the fundamental mode and high order cladding modes through two mismatched sections. It can be done by using a misaligned splice or a short section of a special fiber.

A core offset splice based refractometer was presented by Tian *et al.* [70] (2008). Higher order cladding modes were excited by fusion splicing two singlemode fiber (SMF) sections with a certain core offset. Due to asymmetric nature for a core offset splice, coupling mainly occurs between the $LP_{0,m}$ and $LP_{1,m}$ modes. Two layouts were presented, a Mach-Zehnder by concatenating two misaligned splices and a Michelson, realized by a single core offset splice and a layer of ~ 500nm gold coating at the tip of the optical fiber. The Michelson interferometer was tested as refractometer. The response of the device to external variations of refractive index was evaluated by using dimethyl sulfoxide solutions with different concentrations. The sensitivity for a device with 38 mm of interaction length was 33 nm/RIU in the range of refractive index between 1.315-1.362.

The core-offset technique presents difficulties to control the amount of light power splitting. In alternative, Pang *et al.* [71] presented a Mach-Zehnder based standard SMF sandwiched between two double cladding fibers (DCF) sections. Standard SMF were used for both light input and output of the Mach-Zehnder device. The DCF consists of three layers, the core, inner cladding and external cladding. The inner cladding is thin and its refractive index is lower than that of the core and the external cladding. The DCFs serve as the in-fiber couplers that split and combine light propagating in the core and the outer cladding region. Because of the depressed inner cladding structure, the light wave propagating in the core can be partially coupled to the outer cladding through the evanescent wave. Therefore, the DCF can be employed as a core-cladding modes coupler to construct in-fiber interferometers. The DCF length was approximately 5mm (on both sides), and the interferometer interaction length was 93 mm. Sensitivities of 31 nm/RIU and 823 nm/RIU were obtained for the lower refractive index (1.34 range) and the higher refractive index (1.44 range), respectively.

The idea of fiber a core diameter mismatch (CDM) based interferometer for refractive index sensing has been reported by Rong *et al.* [72]. The sensing probe was constituted by a 9mm section of SMF sandwiched between two 2mm segments of thin core fiber (TCF). The two TCF sections act as core-cladding modes coupling and recoupling, and the SMF middle section performs as the interference arm. The first TCF couples part of the core-guided fundamental mode into forward propagating cladding modes of the downstream SMF via CDM. Thus, the cladding modes propagating in the SMF middle section were sensitive to the SRI. Finally, the

cladding modes are coupled back to the fiber core of lead-out SMF via the second TCF, mixing with the original core mode and generating the interference signal. The studied refractometer exhibited sensitivity up to 159 nm/RIU over low refractive index values from 1.33 to 1.38. Similar work was presented by the same group [73]. Based on the same principle, but using two sections of multimode fiber (MMF) as a core-cladding modes coupling and recoupling mechanism. The sensing probe was constituted by a 40mm section of SMF sandwiched between two 5mm segments of MMF. The device showed sensitivity up to 188 nm/RIU over low RI values from 1.33 to 1.40. Figure 12 shows schematically the MMF assisted Mach-Zehnder interferometer.

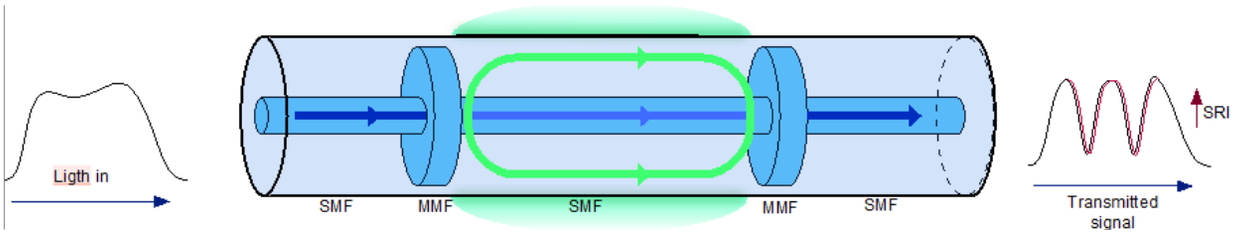

Figure 12. Mach-Zehnder interferometer based on core diameter mismatch

5.3. Multimode interference

Modal interference involving more than two modes has also been studied, resulting into a spectral transfer function that is no co-sinusoidal but instead show sharp peaks at specific wavelengths. It is common to refer this approach as multimode interference (MMI). MMI in optical fiber devices is usually obtained by splicing a MMF section between two single mode fibers, thus forming a SMF-MMF-SMF (SMS) fiber configuration. Based on multimodal interference and the self-imaging or re-imaging effect, the SMS structure acts as an optical band filter that has been widely explored for optical communication and sensing applications.

The SMS fiber concept relies on the fact that when the light field coming from the input SMF enters the MMF, exciting several high order modes, generating a periodic interference pattern along the MMF section. Depending on the wavelength and geometrical length, the light into de MMF can interfere constructively or destructively resulting, at the end, in a device with different spectral characteristics. Therefore the length of the MMF determines the spectral features of the MMI device. Depending where the interference pattern is 'intersected', constructive or destructive interference results, at different wavelengths yielding the transmission of resonant peaks or resonant losses respectively. The transmitted spectral power distribution is, therefore, highly sensitive to the optical path length of the MMF section. It is important to refer that in MMI devices based on standard MMF, the optical signal does not access the external medium. Therefore, they are insensitive to the SRI. MMI based refractometers usually relies on etched cladding MMF, tapered MMF or coreless multimode fibers (CMF). Figure 13 shows conceptually a SMS device based in a CMF, where constructive interference is present resulting in a resonant peak in the transmitted spectrum.

http://dx.doi.org/10.5772/55376

MMI fiber devices are very attractive due to their high potential for refractive index sensing. In 2006, Jung *et al.* [74] presented the first MMI based fiber refractometer. The sensing structure was based in a 125μm diameter coreless silica fiber (CSF) splice between two step index 50/125μm MMF sections. The advantage of use MMF instead SMF is the efficient power coupling and recoupling due to the large core diameter. The refractive index resolution was estimated to be $\pm 4.4\times10^{-4}$ RIU for a refractive index range from 1.30 to 1.44. Later, Wu *et al.* [75] investigated the influence of etched MMF core diameters and on the sensitivity of an SMS fiber based refractometer. They have shown that refractive index sensitivity is highly dependent on the MMF diameter. The SMS fiber structure based refractometer with a core diameter of 80μm has an estimated sensitivity of 180 nm/RIU in the RI range from 1.342 to 1.352 and 1815 nm/RIU in the RI range from 1.431 to 1.437. In another perspective, Biazoli *et al.* [76] studied a tapered SMS structure for high index sensing. The device relies on a coreless MMF, part of which was tapered down by flame brushing technique. For a 55μm MMF taper waist diameter the results showed that in the lower indices range of 1.30–1.33, a sensitivity of 148 nm/RIU was achieved, while in the high sensitivity index region of 1.42–1.43, a value of 2946 nm/RIU was also attained.

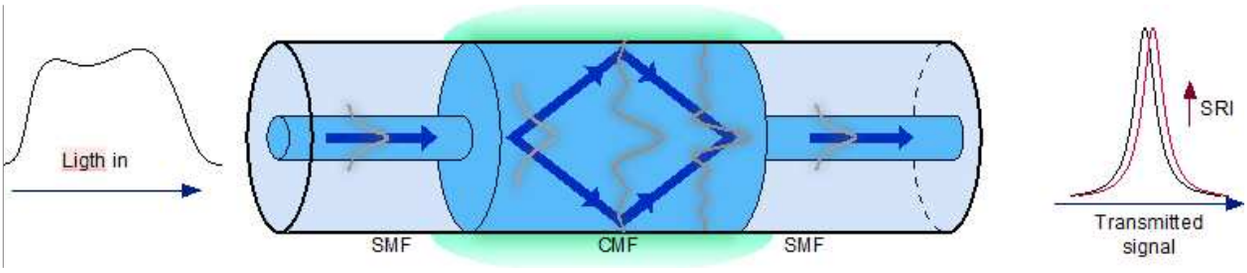

Figure 13. Singlemode-Multimode-Singlemode (SMS) multimodal interferometer

Good sensitivity, ease to fabricate and possibility to build robust devices are some of the advantages of SMS structures for label-free sensing. However, these structures produce a broad optical band spectrum, resulting in a small Q factor and thus poor resolution in the measurement of spectral shift. Concerning improvements in the interrogation schema, Lan *et al.* [77] proposed a SMS fiber structure coated with a zeolite thin film and interrogated by a fiber ring laser for highly sensitive chemical vapor detection. The zeolite-coated SMS structure was used as a bandpass filter and inserted into an Erbium fiber loop to generate a laser line with narrow linewidth and high signal-to-noise ratio. The nanoporous zeolite adsorbs chemical molecules from the surrounding environment to increase its effective refractive index of the coated zeolites, producing a wavelength shift of the SMS filter and a corresponding change in the laser wavelength. The sensor has been demonstrated for detection of ethanol.

A different approach for multimodal interference devices was presented by Xia *et al.* [78]. The authors investigated a fiber modal interferometer constituted by a thin core fiber (TCF) sandwiched between two SMF. The designed TCF modal interferometer was made with a commercial TCF (Nufern 460-HP) whose cut-off wavelength was around three times shorter

than normal SMF. In such structure, the high-order cladding modes will be excited when the light reaches the first heterocore interface. The excited high-order cladding modes will interfere with the core mode at the second heterocore interface due to the existing optical path difference between the two modes. The constructive or destructive interference will determine the output intensity maximum or minimum. Both transmissive and reflective TCF modal interferometers were experimentally demonstrated, and showed a good sensitivity to a small change of external refractive index ~ 100 nm/RIU in the range between 1.34 - 1.39. Gu *et al.* [79] presented a pH sensor based on a TCF modal interferometer with electrostatic self-assembled nanocoating. The surface of the sensor is coated with poly(allylamine hydrochloride) and poly(acrylic acid) nanocoating. A fast and linear response was obtained in either acid or alkali solution (in the pH range 2.5 to 10) with resolution of ±0.013 pH unit.

6. Conclusions

In this chapter a review of evanescent field based refractometric platforms for label free sensing was given. Several aspects regarding the implementation of label free biochemical sensors using standard optoelectronics were address. Different structures were described, including fiber gratings, modal interferometers and multimodal devices. Emphasis was given to the description of fiber optic device and their sensing mechanism, advantages and limitations and the sensing performance of each sensing technology was evaluated. Table 2 summarizes the main features of the refractometric configurations.

Technology	Advantages	Limitations
Etched FBG	Well developed technology Multiplexing capability	Fragility Low sensitivity High cost
Tilted FBG	Well developed technology	Low sensitivity High cost
LPG	High sensitivity	Fabrication Temperature cross-sensitivity
LPG based interferometer	High sensitivity	Fabrication Device length
Abrupt taper	High sensitivity	Fragility
CDM based interferometers	Low-cost	Reproducibility
Multimodal interferometer	Low-cost Low temperature cross-sensitivity	Reproducibility Broader resonance

Table 2. Summary of the advantages and limitation of the studied technologies

http://dx.doi.org/10.5772/55376

Optical fiber gratings, including fiber Bragg gratings and long-period fiber gratings, have also been explored for refractive index sensing. They consist in a periodic modulation of the refractive index of the core of the fiber, where the LPG's period is much longer (hundreds of microns) than the FBG's period (typically a half-wavelength). This structural difference results in devices with fundamentally different properties. FBGs work mainly with radiation confined to the fiber core, in this way strategies have to be devised in order for the radiation to interact with the external medium. Typically, FBG based refractometers rely on the evanescent field of the core mode under fiber etching conditions. FBG based configurations are more attractive for the purpose of multipoint sensing due to their very narrow spectral response. Nevertheless, the etching process introduces fragility in the fiber sensor. Tilted FBGs do not require etching therefore maintain the fiber integrity. Although, a TFBG couples the core mode to a number of cladding modes in a large wavelength bandwidth, it renders difficulty for signal readout and multiplexing. The refractive index sensitivity to these devices (FBG and TFBG) in the biological range is quite low which means that these devices are not very promising for field of biosensing.

Long period gratings (LPG), on the other hand, provide evanescent interaction by exciting cladding modes, and are therefore intrinsically sensitive to external refractive index changes. They maintain fiber integrity and probably represent the most popular device for label free sensing. They present high sensitivity to refractive index measurement, which can be increased and tuned by using HRI overlays. The HRI overlay draws the optical field towards the external medium extending its evanescent wave. As a result there is an increased sensitivity of the device to the SRI. The field enhancement in the overlay depends strongly on the overlay thickness and refractive index. This technique allows the coupling of the optical design and sensitivity optimization of the device, together with the functionalization. The careful design by means the proper choice of the grating period, the overlay RI and a very controlled deposition method, together with the integration on the HRI of sensitive materials or biological active agents, provide a powerful platform for advanced optical label free biochemical sensing. However, LPGs are also highly sensitive to temperature, they need an extra mechanism to compensate temperature changes.

LPG interferometers based on Michelson or Mach-Zehnder layouts or even Fabry-Perot intracavity were also demonstrated showing high sensitivity when compared with single bare LPG, and great potential for the biosensing applications. Nevertheless, the device length (few tens of centimeters) can be a constraint for some applications. Fiber tapers, due its highly reduced cladding diameter have an enhanced evanescent interaction and have long been explored for refractive index measurements by monitoring the transmitted optical power. In spite of high sensitivity and very compact size (few millimeters), however, these structures are very fragile and special packaging is needed.

On the other hand, new configurations using special fibers provide new sensing opportunities. Modal interferometers based on core diameter mismatch, by using thin core fibers or multi-mode fiber used as cladding coupling mechanism have shown good sensitivity, ease of fabrication and potential low cost. Nevertheless, these configurations are difficult to reproduce and to control the mode excitation and the amount of power transferred.

Multimode interference based refractometers are also interesting solutions that rely on the concept of re-imaging effects of MMI patterns present in multimode waveguides. In these devices, the transmitted spectral power distribution is highly sensitive to the optical path length of the multimode fiber and its SRI. Usually based on singlemode-multimode-singlemode structures, they can be easily fabricated and applied in different situations. However, these configurations are also difficult to reproduce and present very broad spectral resonance making for instance multiplexing a very difficult task. The table 2 shows the most relevant evanescent field based fiber refractometers.

Overall, evanescent field fiber refractometers are very attractive due to their immunity to electromagnetic interferences, small size, and capability for in-situ, real-time, remote, and distributed sensing. Most of the applications, however, focus on the measurement of parameters such as the concentration of ethylene glycol, sucrose, salt, ethanol, among others. Nevertheless, this approach is not the most reliable due to the possible interference of other species present in the solution, which are different from the analyte of interest. Thus, the use of sensitive materials containing biomolecules with a natural affinity to the target, or chemical species having analyte specific ligands, has increased, mainly based on LPGs. Several works were reported regarding antibody-antigen interaction and also DNA hybridization. Regarding chemical application several sensing probes were presented to measure pH, Ethanol vapor, ammonia.

Configuration	Measurement method	Sensitivity	Resolution (RIU)	Ref
Microfiber FBG	Spectral Shift	100nm/RIU	-	[10]
TFBG	Spectral Shift	10nm/RIU	10^{-4}	[12]
Bare LPG	Spectral Shift	1481nm/RIU	-	[22]
HRI coated LPG	Spectral Shift	>9000nm/RIU	-	[34]
Mach-Zehnder LPG	Phase	-	$1.8x10^{-6}$	[38]
Fabry-Perot LPG	Spectral Shift	-	$2.1x10^{-5}$	[40]
LPG/FBG	Normalized Optical Power	-	$2x10^{-5}$	[35]
Abrupt Taper	Spectral Shift	1150nm/RIU	$8.2x10^{-6}$	[66]
CDM based Mach-Zehnder	Spectral Shift	188nm/RIU	-	[73]
MMI	Spectral Shift	148nm/RIU	-	[76]

Table 3. Summary of the performance parameters of the most relevant works on fiber based refractometers

Acknowledgements

This work was partially supported by COMPETE program and FCT by funding project n.º FCOMP-01-0124-FEDER-019439 (Refª. FCT PTDC/AGR-ALI/117341/2010). Carlos Gouveia would like to acknowledge the financial support of FCT (SFRH/ BD/ 63758/ 2009)

Author details

Carlos A. J. Gouveia[1,2], Jose M. Baptista[1,2] and Pedro A.S. Jorge[1]

1 INESC-Porto, Rua do Campo Alegre, Porto, Portugal

2 CCCEE, Universidade da Madeira, Campus da Penteada, Funchal, Portugal

References

[1] Hecht, E.: 'Optics 4th edition', Optics 4th edition by Eugene Hecht Reading, MA: Addison-Wesley Publishing Company, 2001, 2001, 1

[2] Fan, X., White, I.M., Shopova, S.I., Zhu, H., Suter, J.D., and Sun, Y.: 'Sensitive optical biosensors for unlabeled targets: A review', Analytica Chimica Acta, 2008, 620, (1-2), pp. 8-26

[3] Kersey, A.D., Davis, M.A., Patrick, H.J., LeBlanc, M., Koo, K.P., Askins, C.G., Putnam, M.A., and Friebele, E.J.: 'Fiber grating sensors', J Lightwave Technol, 1997, 15, (8), pp. 1442-1463

[4] Frazao, O., Ferreira, L.A., Araújo, F.M., and Santos, J.L.: 'Applications of Fiber Optic Grating Technology to Multi-Parameter Measurement', Fiber Integrated Opt, 2005, 24, (3), pp. 227-244

[5] Asseh, A., Sandgren, S., Ahlfeldt, H., Sahlgren, B., Stubbe, R., and Edwall, G.: 'Fiber optical Bragg grating refractometer', Fiber Integrated Opt, 1998, 17, (1), pp. 51-62

[6] Schroeder, K., Ecke, W., Mueller, R., Willsch, R., and Andreev, A.: 'A fibre Bragg grating refractometer', Meas Sci Technol, 2001, 12, (7), pp. 757-764

[7] Iadicicco, A., Campopiano, S., Cutolo, A., Giordano, M., and Cusano, A.: 'Nonuniform thinned fiber Bragg gratings for simultaneous refractive index and temperature measurements', Photonics Technology Letters, IEEE, 2005, 17, (7), pp. 1495-1497

[8] Chryssis, A.N., Lee, S.M., Lee, S.B., Saini, S.S., and Dagenais, M.: 'High sensitivity evanescent field fiber Bragg grating sensor', Photonics Technology Letters, IEEE, 2005, 17, (6), pp. 1253-1255

[9] Fang, X., Liao, C.R., and Wang, D.N.: 'Femtosecond laser fabricated fiber Bragg grating in microfiber for refractive index sensing', Optics Letters, 2010, 35, (7), pp. 1007-1009

[10] Zhang, Y., Lin, B., Tjin, S.C., Zhang, H., Wang, G., Shum, P., and Zhang, X.: 'Refractive index sensing based on higher-order mode reflection of a microfiber Bragg grating', Opt Express, 2010, 18, (25), pp. 26345-26350

[11] Laffont, G., and Ferdinand, P.: 'Tilted short-period fibre-Bragg-grating-induced coupling to cladding modes for accurate refractometry', Meas Sci Technol, 2001, 12, (7), pp. 765-770

[12] Chan, C.-F., Chen, C., Jafari, A., Laronche, A., Thomson, D.J., and Albert, J.: 'Optical fiber refractometer using narrowband cladding-mode resonance shifts', Appl Optics, 2007, 46, (7), pp. 1142-1149

[13] Han, M., Guo, F., and Lu, Y.: 'Optical fiber refractometer based on cladding-mode Bragg grating', Optics Letters, 2010, 35, (3), pp. 399-401

[14] Wu, Q., Semenova, Y., Yan, B., Ma, Y., Wang, P., Yu, C., and Farrell, G.: 'Fiber refractometer based on a fiber Bragg grating and single-mode-multimode-single-mode fiber structure', Optics Letters, 2011, 36, (12), pp. 2197-2199

[15] Liang, W., Huang, Y., Xu, Y., Lee, R.K., and Yariv, A.: 'Highly sensitive fiber Bragg grating refractive index sensors', Appl Phys Lett, 2005, 86, (15), pp. 151122-151122

[16] Chryssis, A.N., Saini, S.S., Lee, S.M., Yi, H.M., Bentley, W.E., and Dagenais, M.: 'Detecting hybridization of DNA by highly sensitive evanescent field etched core fiber bragg grating sensors', IEEE Journal of Selected Topics in Quantum Electronics, 2005, 11, (4), pp. 864-872

[17] Maguis, S., Laffont, G., Ferdinand, P., Carbonnier, B., Kham, K., Mekhalif, T., and Millot, M.-C.: 'Biofunctionalized tilted Fiber Bragg Gratings for label-free immunosensing', Opt Express, 2008, 16, (23), pp. 19049-19062

[18] James, S., and Tatam, R.: 'Optical fibre long-period grating sensors: Characteristics and application', Measurement Science and Technology, 2003, 14, (5), pp. R49-R61

[19] Erdogan, T.: 'Cladding-mode resonances in short- and long-period fiber grating filters', Journal of the Optical Society of America a-Optics Image Science and Vision, 1997, 14, (8), pp. 1760-1773

[20] Vengsarkar, A.M., Lemaire, P.J., Judkins, J.B., Bhatia, V., Erdogan, T., and Sipe, J.E.: 'Long-period fiber gratings as band-rejection filters', Lightwave Technology, Journal of, 1996, 14, (1), pp. 58-65

[21] Bhatia, V., and Vengsarkar, A.M.: 'Optical fiber long-period grating sensors', Optics Letters, 1996, 21, (9), pp. 692-694

[22] Shu, X., Zhang, L., and Bennion, I.: 'Sensitivity characteristics of long-period fiber gratings', Lightwave Technology, Journal of, 2002, 20, (2), pp. 255-266

[23] Smietana, M., Bock, W.J., Mikulic, P., and Chen, J.: 'Increasing sensitivity of arc-induced long-period gratings—pushing the fabrication technique toward its limits', Measurement Science and Technology, 2010, 22, (1), pp. 015201

[24] Rees, N., James, S., and Tatam, R.: 'Optical fiber long-period gratings with Langmuir—Blodgett thin-film overlays', Optics Letters, 2002, 27, (9), pp. 686-688

[25] Cusano, A., Iadicicco, A., Pilla, P., Contessa, L., Campopiano, S., Cutolo, A., Giordano, M., and Guerra, G.: 'Coated long-period fiber gratings as high-sensitivity optochemical sensors', Lightwave Technology, Journal of, 2006, 24, (4), pp. 1776-1786

[26] Del Villar, I., Matias, I., and Arregui, F.: 'Optimization of sensitivity in long period fiber gratings with overlay deposition', Opt Express, 2005, 13, (1), pp. 56-69

[27] Ishaq, I., Quintela, A., James, S., Ashwell, G., Lopez-Higuera, J., and Tatam, R.: 'Modification of the refractive index response of long period gratings using thin film overlays', Sensor Actuat B-Chem, 2005, 107, (2), pp. 738-741

[28] Pilla, P., Giordano, M., Korwin-Pawlowski, M.L., Bock, W.J., and Cusano, A.: 'Sensitivity Characteristics Tuning in Tapered Long-Period Gratings by Nanocoatings', Ieee Photonic Tech L, 2007, 19, (19), pp. 1517-1519

[29] Corres, J.M., Matias, I.R., del Villar, I., and Arregui, F.J.: 'Design of pH Sensors in Long-Period Fiber Gratings Using Polymeric Nanocoatings', IEEE Sensors Journal, 2007, 7, (3), pp. 455-463

[30] Gu, Z., and Xu, Y.: 'Design optimization of a long-period fiber grating with sol-gel coating for a gas sensor', Measurement Science and Technology, 2007, 18, (11), pp. 3530-3536

[31] Cusano, A., Iadicicco, A., Pilla, P., Contessa, L., Campopiano, S., Cutolo, A., and Giordano, M.: 'Mode transition in high refractive index coated long period gratings', Opt Express, 2006, 14, (1), pp. 19

[32] Pilla, P., Manzillo, P.F., Malachovska, V., Buosciolo, A., Campopiano, S., Cutolo, A., Ambrosio, L., Giordano, M., and Cusano, A.: 'Long period grating working in transition mode as promising technological platform for label-free biosensing', Opt Express, 2009, 17, (22), pp. 20039-20050

[33] Patrick, H.J., Kersey, A.D., and Bucholtz, F.: 'Analysis of the response of long period fiber gratings to external index of refraction', J Lightwave Technol, 1998, 16, (9), pp. 1606-1612

[34] Pilla, P., Trono, C., Baldini, F., Chiavaioli, F., Giordano, M., and Cusano, A.: 'Giant sensitivity of long period gratings in transition mode near the dispersion turning point: an integrated design approach', Optics Letters, 2012, 37, (19), pp. 4152-4154

[35] Jesus, C., Caldas, P., Frazao, O., Santos, J.L., Jorge, P.A.S., and Baptista, J.M.: 'Simultaneous Measurement of Refractive Index and Temperature Using a Hybrid Fiber Bragg Grating/Long-Period Fiber Grating Configuration', Fiber Integrated Opt, 2009, 28, (6), pp. 440-449

[36] Baldini, F., Brenci, M., Chiavaioli, F., Giannetti, A., and Trono, C.: 'Optical fibre gratings as tools for chemical and biochemical sensing', Anal Bioanal Chem, 2012, 402, (1), pp. 109-116

[37] Duhem, O., Henninot, J.F., and Douay, M.: 'Study of in fiber Mach-Zehnder interferometer based on two spaced 3-dB long period gratings surrounded by a refractive index higher than that of silica', Optics Communications, 2000, 180, (4), pp. 255-262

[38] Allsop, T., Reeves, R., Webb, D.J., Bennion, I., and Neal, R.: 'A high sensitivity refractometer based upon a long period grating Mach-Zehnder interferometer', Rev Sci Instrum, 2002, 73, (4), pp. 1702-1705

[39] Swart, P.L.: 'Long-period grating Michelson refractometric sensor', Meas Sci Technol, 2004, 15, (8), pp. 1576-1580

[40] Mosquera, L., Saez-Rodriguez, D., Cruz, J.L., and Andres, M.V.: 'In-fiber Fabry-Perot refractometer assisted by a long-period grating', Optics Letters, 2010, 35, (4), pp. 613-615

[41] Falciai, R., Mignani, A.G., and Vannini, A.: 'Long period gratings as solution concentration sensors'. Proc. Sensor Actuat B-Chem2001 pp. Pages

[42] Allsop, T., Zhang, L., and Bennion, I.: 'Detection of organic aromatic compounds in paraffin by a long-period fiber grating optical sensor with optimized sensitivity', Optics Communications, 2001, 191, pp. 181-190

[43] Tang, J.-L., Cheng, S.-F., Hsu, W.-T., Chiang, T.-Y., and Chau, L.-K.: 'Fiber-optic biochemical sensing with a colloidal gold-modified long period fiber grating', Sensor Actuat B-Chem, 2006, 119, (1), pp. 105-109

[44] Possetti, G.R.C., Kamikawachi, R.C., Prevedello, C.L., Muller, M., and Fabris, J.L.: 'Salinity measurement in water environment with a long period grating based interferometer', Measurement Science and Technology, 2009, 20, (3), pp. 4003

[45] Manzillo, P.F., Pilla, P., Buosciolo, A., Campopiano, S., Cutolo, A., Borriello, A., Giordano, M., and Cusano, A.: 'Self Assembling and Coordination of Water Nano-Layers On Polymer Coated Long Period Gratings: Toward New Perspectives for Cation Detection', Soft Materials, 2011, 9, (2-3), pp. 238-263

[46] Li, Q., Zhang, X.-l., Yu, Y.-S., Qian, Y., Dong, W.-F., Li, Y., Shi, J., Yan, J., and Wang, H.: 'Enhanced sucrose sensing sensitivity of long period fiber grating by self-assembled polyelectrolyte multilayers', Reactive and Functional Polymers, 2011, 71, (3), pp. 335-339

[47] Barnes, J., Dreher, M., Plett, K., Brown, R.S., Crudden, C.M., and Loock, H.-P.: 'Chemical sensor based on a long-period fibre grating modified by a functionalized polydimethylsiloxane coating', The Analyst, 2008, 133, (11), pp. 1541-1549

[48] Barnes, J.A., Brown, R.S., Cheung, A.H., Dreher, M.A., Mackey, G., and Loock, H.-P.: 'Chemical sensing using a polymer coated long-period fiber grating interrogated by ring-down spectroscopy', Sensor Actuat B-Chem, 2010, 148, (1), pp. 221-226

[49] Zhang, J., Tang, X., Dong, J., Wei, T., and Xiao, H.: 'Zeolite thin film-coated long period fiber grating sensor for measuring trace chemical', Opt Express, 2008, 16, (11), pp. 8317-8323

[50] Korposh, S., Selyanchyn, R., Yasukochi, W., Lee, S.-W., James, S.W., and Tatam, R.P.: 'Optical fibre long period grating with a nanoporous coating formed from silica nanoparticles for ammonia sensing in water', Materials Chemistry and Physics, 2012, 133, pp. 784-792

[51] DeLisa, M.P., Zhang, Z., Shiloach, M., Pilevar, S., Davis, C.C., Sirkis, J.S., and Bentley, W.E.: 'Evanescent Wave Long-Period Fiber Bragg Grating as an Immobilized Antibody Biosensor', Analytical Chemistry, 2000, 72, (13), pp. 2895-2900

[52] Kim, D., Zhang, Y., Cooper, K., and Wang, A.: 'In-fiber reflection mode interferometer based on a long-period grating for external refractive-index measurement', Appl Optics, 2005, 44, (26), pp. 5368-5373

[53] Yang, J., Sandhu, P., Liang, W., Xu, C.Q., and Li, Y.: 'Label-free fiber optic biosensors with enhanced sensitivity', Selected Topics in Quantum Electronics, IEEE Journal of, 2007, 13, (6), pp. 1691-1696

[54] Wang, Z., Heflin, J.R., Van Cott, K., Stolen, R.H., Ramachandran, S., and Ghalmi, S.: 'Biosensors employing ionic self-assembled multilayers adsorbed on long-period fiber gratings', Sensor Actuat B-Chem, 2009, 139, (2), pp. 618-623

[55] Wang, Z., and Xiao, H.: 'Optical intensity-based long-period fiber grating biosensors and biomedical applications [Life Sciences]', Signal Processing Magazine, IEEE, 2009, 26, (2), pp. 121-122, 124-127

[56] Wang, D.Y., Wang, Y., Han, M., Gong, J., and Wang, A.: 'Fully Distributed Fiber-Optic Biological Sensing', Ieee Photonic Tech L, 2010, 22, (21), pp. 1553-1555

[57] Pilla, P., Malachovská, V., Borriello, A., Buosciolo, A., Giordano, M., Ambrosio, L., Cutolo, A., and Cusano, A.: 'Transition mode long period grating biosensor with functional multilayer coatings', Opt Express, 2011, 19, (2), pp. 512

[58] Cooper, K.L., Bandara, A.B., Wang, Y., Wang, A., and Inzana, T.J.: 'Photonic Biosensor Assays to Detect and Distinguish Subspecies of Francisella tularensis', Sensors, 2011, 11, (3), pp. 3004-3019

[59] Pilla, P., Sandomenico, A., Malachovská, V., Borriello, A., Giordano, M., Cutolo, A., Ruvo, M., and Cusano, A.: 'A protein-based biointerfacing route toward label-free immunoassays with long period gratings in transition mode', Biosensors and Bioelectronics, 2012, 31, (1), pp. 486-491

[60] Chen, X., Zhang, L., Zhou, K., Davies, E., Sugden, K., Bennion, I., Hughes, M., and Hine, A.: 'Real-time detection of DNA interactions with long-period fiber-grating-based biosensor', Optics Letters, 2007, 32, (17), pp. 2541

[61] Jang, H.S., Park, K.N., Kim, J.P., Sim, S.J., Kwon, O.J., Han, Y.-G., and Lee, K.S.: 'Sensitive DNA biosensor based on a long-period grating formed on the side-polished fiber surface', Opt Express, 2009, 17, (5), pp. 3855

[62] Hine, A.V., Chen, X., Hughes, M.D., Zhou, K., Davies, E., Sugden, K., Bennion, I., and Zhang, L.: 'Optical fibre-based detection of DNA hybridization', Biochem Soc Trans, 2009, 37, (Pt 2), pp. 445-449

[63] Smietana, M., Bock, W.J., Mikulic, P., Ng, A., Chinnappan, R., and Zourob, M.: 'Detection of bacteria using bacteriophages as recognition elements immobilized on long-period fiber gratings', Opt Express, 2011, 19, (9), pp. 7971

[64] Tripathi, S.M., Bock, W.J., Mikulic, P., Chinnappan, R., Ng, A., Tolba, M., and Zourob, M.: 'Long period grating based biosensor for the detection of Escherichia coli bacteria', Biosensors and Bioelectronics, 2012, 35, (1), pp. 308-312

[65] Deep, A., Tiwari, U., Kumar, P., Mishra, V., Jain, S.C., Singh, N., Kapur, P., and Bharadwaj, L.M.: 'Immobilization of enzyme on long period grating fibers for sensitive glucose detection', Biosensors and Bioelectronics, 2012, 33, (1), pp. 190-195

[66] Zibaii, M.I., Latifi, H., Karami, M., Gholami, M., Hosseini, S.M., and Ghezelayagh, M.H.: 'Non-adiabatic tapered optical fiber sensor for measuring the interaction between alpha-amino acids in aqueous carbohydrate solution', Meas Sci Technol, 2010, 21, (10)

[67] Zibaii, M.I., Kazemi, A., Latifi, H., Azar, M.K., Hosseini, S.M., and Ghezelaiagh, M.H.: 'Measuring bacterial growth by refractive index tapered fiber optic biosensor', J Photoch Photobio B, 2010, 101, (3), pp. 313-320

[68] Zibaii, M.I., Frazao, O., Latifi, H., and Jorge, P.A.S.: 'Controlling the Sensitivity of Refractive Index Measurement Using a Tapered Fiber Loop Mirror', Photonics Technology Letters, IEEE, 2011, 23, (17), pp. 1219-1221

[69] Tian, Y., Wang, W., Wu, N., Zou, X., and Wang, X.: 'Tapered Optical Fiber Sensor for Label-Free Detection of Biomolecules', Sensors, 2011, 11, (4), pp. 3780-3790

[70] Tian, Z., Yam, S.S.H., and Loock, H.-P.: 'Single-Mode Fiber Refractive Index Sensor Based on Core-Offset Attenuators', Ieee Photonic Tech L, 2008, 20, (16), pp. 1387-1389

[71] Pang, F.F., Liu, H.H., Guo, H.R., Liu, Y.Q., Zeng, X.L., Chen, N., Chen, Z.Y., and Wang, T.Y.: 'In-Fiber Mach-Zehnder Interferometer Based on Double Cladding Fibers for Refractive Index Sensor', IEEE Sensors Journal, 2011, 11, (10), pp. 2395-2400

[72] Rong, Q., Qiao, X., Wang, R., Sun, H., Hu, M., and Feng, Z.: 'High-Sensitive Fiber-Optic Refractometer Based on a Core-Diameter-Mismatch Mach-Zehnder Interferometer', IEEE Sensors Journal, 2012, 12, (7), pp. 2501-2505

[73] Ma, Y., Qiao, X., Guo, T., Wang, R., Zhang, J., Weng, Y., Rong, Q., Hu, M., and Feng, Z.: 'Mach–Zehnder Interferometer Based on a Sandwich Fiber Structure for Refractive Index Measurement', IEEE Sensors Journal, 2012, 12, (6), pp. 2081-2085

[74] Jung, Y., Kim, S., Lee, D., and Oh, K.: 'Compact three segmented multimode fibre modal interferometer for high sensitivity refractive-index measurement', Meas Sci Technol, 2006, 17, (5), pp. 1129-1133

[75] Wu, Q., Semenova, Y., Wang, P., and Farrell, G.: 'High sensitivity SMS fiber structure based refractometer - analysis and experiment', Opt Express, 2011, 19, (9), pp. 7937-7944

[76] Biazoli, C.R., Silva, S., Franco, M.A., Frazao, O., and Cordeiro, C.M.: 'Multimode interference tapered fiber refractive index sensors', Appl Opt, 2012, 51, (24), pp. 5941-5945

[77] Lan, X., Huang, J., Han, Q., Wei, T., Gao, Z., Jiang, H., Dong, J., and Xiao, H.: 'Fiber ring laser interrogated zeolite-coated singlemode-multimode-singlemode structure for trace chemical detection', Optics Letters, 2012, 37, (11), pp. 1998-2000

[78] Xia, T.-H., Zhang, A.P., Gu, B., and Zhu, J.-J.: 'Fiber-optic refractive-index sensors based on transmissive and reflective thin-core fiber modal interferometers', Optics Communications, 2010, 283, (10), pp. 2136-2139

[79] Gu, B., Yin, M.J., Zhang, A.P., Qian, J.W., and He, S.: 'Low-cost high-performance fiber-optic pH sensor based on thin-core fiber modal interferometer', Opt Express, 2009, 17, (25), pp. 22296-22302

IntechOpen